

ASH DEPOSITION BEHAVIOR OF A COAL, A CLEAN COAL, AND A CHAR IN A DROP TUBE FURNACE

M. Rostam-Abadi, J.A. DeBarr, and R.D. Harvey

Illinois State Geological Survey
615 E. Peabody Drive
Champaign, IL 61820

Keywords: ash deposition, mild gasification char, drop tube furnace

INTRODUCTION

This work was undertaken as part of a larger study to evaluate the combustion characteristics of chars derived from Illinois coals under mild gasification (MG) conditions. The principle product (60 to 70 percent by weight) of MG processes is a char that must be effectively utilized to improve the overall economics of the process. During the past several years, one of the major research activities at the Illinois State Geological Survey has been to examine the suitability of using MG char as a fuel, alone or as coal-char blend, in typical industrial pulverized-coal (PC) boilers. The physical and chemical characteristics and reactivity of laboratory- and pilot plant-prepared MG chars have been reported (1-4).

In this paper preliminary results of a study to evaluate the ash deposition behavior of an MG char under conditions representative of PC boilers are presented. The results are compared to those obtained with the raw coal and a physically cleaned coal. Ash deposition tests were performed in a laminar flow (drop tube) furnace.

EXPERIMENTAL

Sample Preparation - The clean coal and the char were made from an original sample of the Herrin coal seam (IL No. 6) that was provided by the Illinois Basin Coal Sample Program, identified as IBC-101 (5). The parent sample represented the product from the mines preparation plant. The analysis of the coal is given in table 1.

The clean coal was prepared from a 200x400 mesh size fraction of the original coal in a Denver model D-2 batch flotation system. Approximately 150 grams of coal was combined with four liters of water in the flotation cell. A flotation agent (2-ethyl hexanol) was added at an equivalence of 6 lbs/ton. Additional ash was removed by repeating the procedure using the clean coal as the starting material. The clean coal was vacuum filtered, dried in a vacuum oven at 80 °C, and stored under nitrogen to prevent oxidation. The analysis of the product sample is given in table 1. The amount of ash in the clean coal is 6.4% which corresponds to a 34% decrease compared to the parent (200x400 mesh) coal. However, the clean coal retains almost 87% of the sulfur present in the original coal. This is because 72% of the sulfur in the parent coal is in the form of organic sulfur which is not removed by flotation methods.

A 5.1 cm ID batch fluidized-bed reactor system was used for the production of the char. The sample used for char production was a 28x100 mesh size fraction of the coal. In each run, about 200 grams of the coal was fluidized by nitrogen flowing at 6 l/min and heated according to a multi-step heating procedure to minimize agglomeration of coal particles in the reactor. The final temperature and final soak time were adjusted to produce three chars with volatile matter contents of about 7, 12, and 15%. The 7% volatile char was selected for ash deposition studies because it had higher ash content (14.1%, see table 1) than the other chars. The final temperatures and soak times for the char were 600 °C and 60 mins. After the final soak, the samples were cooled under

nitrogen purge and stored under nitrogen.

Ash Characteristics - The ash compositions (major and minor oxides) were determined by routine methods, and the ash fusability temperatures of the coal, clean coal, and char were determined by the ASTM D1857 method. These data were used to calculate silica ratio, base/acid ratio, T_c (temperature at critical viscosity), T_{250} (temperature at which the slag has a viscosity of 250 poise), the viscosity of slag at 2600 °F and the slugging index and fouling index.

Ash Deposition Studies - Ash deposition tests were conducted in a drop tube furnace (DTF) located at the University of North Dakota's Energy and Environmental Research Center (UNDEERC). The DTF is described elsewhere (6). A brief description of the ash deposition probe follows.

The water-cooled ash deposition probe, shown in figure 1, consists of a 2.2 cm OD stainless steel tube with a 3.8 cm OD diameter cap. A machined, boiler-steel substrate plate (3.8 cm diameter by 0.64 cm thick) prepared from 1040 carbon steel, supplied by the Babcock and Wilcox Company, is attached to the top of the probe. The substrate plate temperature can be maintained between 350 to 540 °C to simulate a boiler heat transfer surface, by adjusting cooling water and the tightness of the screws that hold the substrate to the probe. The temperature is monitored by a Type K thermocouple in contact with the plate. The substrate plates were polished with SiC polishing discs starting at 120 grit and proceeding to 600 grit. The substrates were oxidized at 400 °C for 20 hours in air to produce an oxide layer on the steel.

In each test, the drop tube furnace was stabilized at 1500 °C and the nominal gas flow rates of 1 l/min primary gas flow and 3 l/min secondary gas flow. The sample feeder was loaded with the desired sample, and the feed rate adjusted to give approximately 0.2 g/min. After the test run, the probe was allowed to cool and the substrate with the ash deposit removed and stored pending strength tests on the ash deposit. The strength of the deposits formed in the DTF were measured using a strength testing apparatus. The strength testing apparatus is described elsewhere (6).

RESULTS

Ash Characteristics - Analyses of the ash from these samples showed only small differences between the coals and char (table 2). The cleaning process removed soluble sulfate minerals, and about half the calcite. The clay minerals and quartz were retained in the clean coal. The temperature for which the ash achieves the desired viscosity of 250 poise (T_{250} , table 3) ranged from 2030 °F (clean coal) to 2115 °F (char). Experience indicates values below 2600 °F are desirable (7).

Slugging indices for the three samples fell in the medium range, according to Attig and Duzy (8), while the fouling index was high for the feed coal and char samples and medium for the clean coal (table 3).

Ash deposition studies - The results of the ash deposition tests are shown in table 4. The ash weight was normalized to a feed rate of 0.13 g/min. This gave a basis to compare the different tests. Clean coal produced about 50% more deposit than the parent coal (figure 2). However, the parent coal and clean coal gave deposit weight curves with similar slopes. Ash deposit weights of the char were substantially higher than either coal or clean coal.

The deposit weight for the clean coal increased faster than that of the parent coal in spite of the fact that it contains about two-thirds the ash of coal (9.7% vs. 6.4%). Without a detailed mineral analysis of the deposits, it is difficult to determine the cause of this behavior. Because the cleaning process removed a portion of the original

mineral matter (particularly calcite, see table 2), altering the composition of the remaining ash, the new composition may have resulted in a "stickier" ash with a higher melting point than the original ash. The ash deposition behavior of the char is consistent with its high ash content (14.1%).

The deposit growth rate curves were used to calculate sticking coefficients. The sticking coefficient (SC) is defined as:

$$SC = \text{rate of ash deposition/rate of firing of ASTM ash}$$

where "ASTM ash" is the ash yield of the fuel as determined by the standard ASTM proximate analysis procedure, or in this study, by TGA analysis of the fuel. The sticking coefficient is a normalized measure of how much ash in the fuel is sticking to the substrate plate of the ash deposition probe, and has a value between zero and one. A value of zero indicates that none of the ash is sticking; a value of one indicates that all of the ash is sticking. The higher the value of the sticking coefficient, the more slagging and fouling are likely to occur.

The deposit rates were calculated from best-fit curves that were determined using the deposit weight and time (table 4). For the parent coal and clean coal, a quadratic equation was fitted to the deposit weight data. It was not possible to obtain a meaningful quadratic equation to fit the data for the char. The instantaneous deposit rates were divided by the ASTM ash firing rate to give the sticking coefficients. The data indicate that the clean coal deposits grew at a faster rate than the parent coal (figure 3). While it was not possible to determine a numerical sticking coefficient for char, the normalized deposit weight data presented in table 4 show that the sticking coefficient for char is high, indicating that the deposits from the char grew much faster than those of the coal samples.

The differences observed in the sticking coefficients for the parent coal and clean coal are likely related to the association of the inorganic constituents in the coal. The inorganic components in the clean coal occur within and/or with carbonaceous particles because the cleaning process removes much of the extraneous (or carbon free) mineral grains. During combustion, the inorganic components associated with coal particles are subjected to higher temperatures than extraneous mineral grains. As a result of the higher temperatures, more of the particles melt and are sticky when they reach the deposition probe, producing a higher sticking coefficient. It is also possible that the included minerals are collected on the surface of the extraneous mineral particles (those deposited on the probe) and carry off the probe by the extraneous mineral particles.

The deposit strength curves are shown in figure 4. Clean coal has a gradual slope to the deposit strength curve and is lower in strength than the coal. The parent coal has an initial slope similar to that of clean coal, but the strength increases rapidly near the top of the deposit. The deposit strength of char exceeded the maximum capacity of the test apparatus (100 psi) and was not included in figure 4.

The difference in the strength of the deposits produced from the parent and cleaned coals is probably due to the types of ash particles in deposits. The strength of the clean coal deposits was lower than the other samples because some of the reactive, liquid producing ash components were removed by cleaning. For example, during the cleaning process a significant amount of pyrite is removed. The iron in pyrite, when combined with aluminosilicates in a combustion environment, produces low melting-temperature phases that are responsible for greater deposit strengths. The greater amount of iron present in the parent coal probably caused the parent coal's stronger deposits. The deposits produced from the clean coal most likely did not contain sufficient fluxing agents such as iron to develop high strength.

Physically, the deposits left by the clean coal were not molten whereas the deposits left by the coal were molten near the top. The deposits left by the char were molten not only at the top but also down the center of the deposit. Melting of deposits increases their strength; this explains the high strength of the char deposits.

CONCLUSIONS

The ash deposition behavior of an Illinois Herrin (No. 6) coal, and of a clean coal product, and a char derived from the parent coal was evaluated. The deposits were collected on a water-cooled stainless steel probe located inside an entrained flow reactor operating at 1500 °C and 20% oxygen. Standard ASTM analyses showed only small differences between the composition of the coal and char ashes; however, the clean coal had substantially lower soluble sulfate minerals and calcite than the coal. Ash deposition studies in a DTF showed that although the clean coal produced a larger deposit that grew at a faster rate than that of the original coal, the clean coal deposits were weaker than those of the coal and showed evidence of partial melting. The deposits from the char grew much faster than that of either the coal or clean coal. Due to extensive melting, the deposits formed by the char were much stronger than those of either the parent coal or clean coal.

ACKNOWLEDGEMENTS

This work was sponsored by The Illinois Department of Energy and Natural Resources through its Coal Development Board and Center for Research on Sulfur in Coal. We thank Dr. S. A. Benson, Mr. D. L. Toman, and Dr. D. P. McCollor for coordinating DTF tests at EERC.

REFERENCES

1. Rostam-Abadi, M., J.A. DeBarr, and W.T. Chen, 1989. ACS, Div. Fuel Chem., prep., 35 (4), pg. 1264-71.
2. Rostam-Abadi, M., J.A. DeBarr, and W.T. Chen, 1990. Thermochemica Acta, 116, pg. 351-356.
3. Rostam-Abadi, M., J.A. DeBarr, and W.T. Chen, 1992. To be published in Thermochemica Acta.
4. DeBarr, J.A., M. Rostam-Abadi, and C.W. Kruse, 1992. ACS Div. Fuel Chem., prep, General Papers, San Francisco, CA, April 5-10.
5. Harvey, R.D. and C.W. Kruse, 1988. J. of Coal Quality, 7 (4), pg. 109-112.
6. Toman, D.L., D.P. McCollor, and S.A. Benson, 1991. Annual Technical Progress Report submitted to ISGS and U.S. DOE.(PETC), EERC, University of North Dakota.
7. Babcock & Wilcox, 1972. Steam - its generation and use. Babcock & Wilcox, New York, NY, pg. 4-15.
8. Attig, R.C. and A.F. Dazy, 1969. Proceedings, Am. Power Conference, 31, pg. 290-300.

Table 1. Proximate and ultimate analysis for samples (dry basis)

Particle Size Mesh	270x400 Parent Coal	200x400 Clean Coal	270x400 Char
Moisture	2.9	1.6	0.9
<u>Proximate, wt%^a</u>			
Volatile Matter	41.8	41.5	7.3
Fixed Carbon	48.5	52.2	78.9
H-T Ash	9.7	6.3	13.8
<u>Ultimate, wt%^b</u>			
Hydrogen	5.2	5.5	2.2
Carbon	69.5	73.3	78.2
Nitrogen	1.5	1.8	2.2
Oxygen ^c	9.5	9.8	1.1
Sulfur	4.6	4.0	2.9
BTU/lb	12674	13293	12791
lb SO ₂ /MMBTU	7.2	6.0	4.6

^a TGA analysis, ^b LECO CHN 600 analyzer, ^c determined by difference

Table 2. Ash composition

Oxide	Parent Coal*	Clean Coal	Char
<u>Ash Analyses (% of ash)</u>			
SiO ₂	48.60	49.30	48.20
Al ₂ O ₃	17.49	17.81	17.36
Fe ₂ O ₃	18.22	19.53	18.08
CaO	4.89	2.20	4.76
MgO	0.99	1.31	0.98
K ₂ O	2.22	2.37	2.22
Na ₂ O	1.47	1.11	1.50
TiO ₂	0.89	1.34	0.90
P ₂ O ₅	0.27	0.14	0.26
MnO ₂	0.05	0.04	0.06
SrO	0.04	0.05	0.04
BaO	0.04	0.05	0.04
SO ₃	4.19	1.94	4.29
Silica ratio	68.85	68.15	66.93
Base/acid	0.41	0.39	0.41

*Mineral matter in IBC-101: 2.6% quartz, 0.5% calcite, 2.1% pyrite and Marcasite, 3.3% kaolinite, 2.4% illite, and 2.1% expandable clay.

Table 3. Ash fusability temperatures

	Parent Coal	Clean Coal	Char
<u>Ash Fusion ('F, reducing)</u>			
Initial def.	2055	2030	2115
Softening	2140	2140	2185
Hemispheric	2225	2245	2260
Fluid	2310	2350	2330
<u>Empirical ash properties</u>			
T ₂₅₀ , 'F	2425	2480	2460
T _{cv} , 'F	2584	2558	2584
Slag viscosity (poise) @2600 'F	105	125	106
Slagging index	1.75	1.53	1.20
type	med.	med.	med.
Fouling index	0.60	0.43	0.62
type	high	medium	high

Table 4. Ash deposition weights

Sample	Time (min)	Coal fed (g)	Ash (g)	Normalized ash (g)
Char	10	0.78	0.0619	0.1032
	20	2.70	0.2669	0.2570
	30	3.68	0.2618	0.2775
Parent coal	10	1.48	0.0488	0.0429
	20	2.24	0.0650	0.0754
	30	3.52	0.1029	0.1140
Clean coal	10	0.90	0.0463	0.0669
	20	3.81	0.1438	0.0981
	30	2.83	0.1070	0.1475

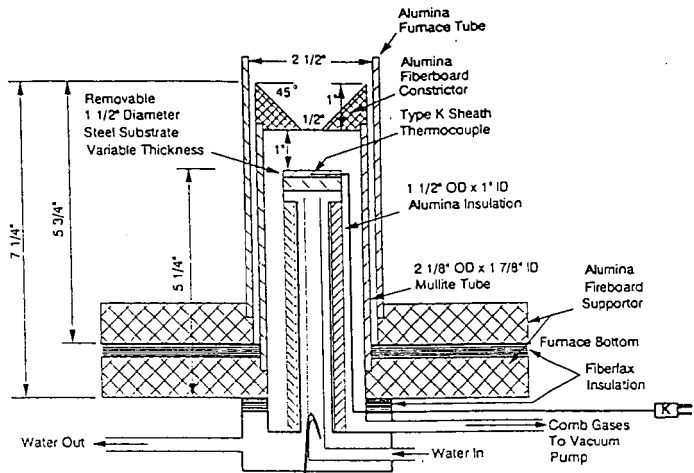


Figure 1. Ash deposition probe.

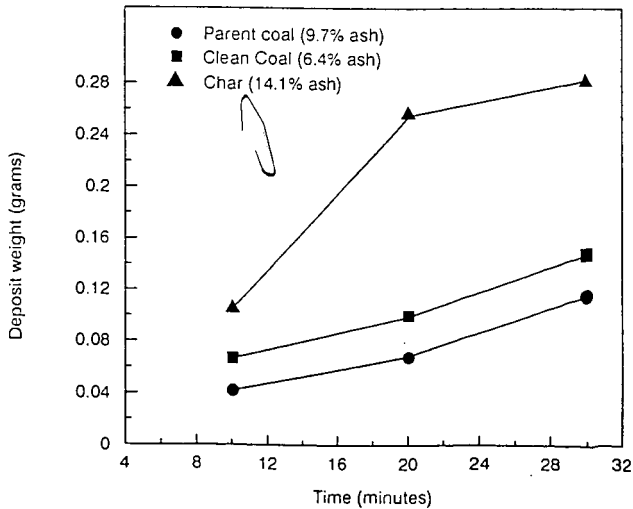


Figure 2. Deposit growth rates for fuels ($T = 1500^{\circ}\text{C}$)

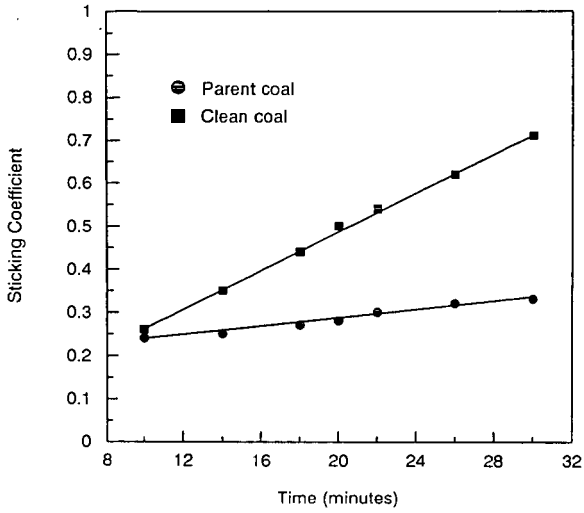


Figure 3. Sticking coefficients for coal samples.

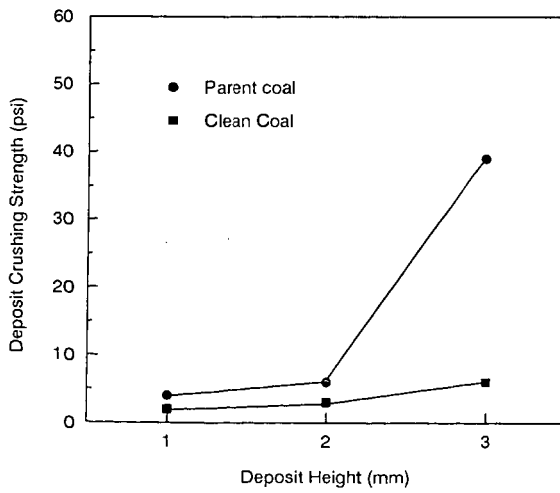


Figure 4. Deposit crushing strength for coal samples.

PROPERTIES OF MILD GASIFICATION CHAR: A COMPARISON OF PILOT PLANT- AND LABORATORY-PREPARED SAMPLES

J. A. DeBarr, M. Rostam-Abadi, R. D. Harvey and C. W. Kruse,
Illinois State Geological Survey, Champaign, IL

Keywords: mild gasification, pyrolysis, coal-char blend

INTRODUCTION

Mild gasification (MG) of high volatile bituminous coal to produce high quality liquid, solid and gaseous products has been a major coal research activity at the Illinois State Geological Survey (ISGS) since 1986. Three major foci of the program have been to 1) evaluate conditions for producing the highest quality liquids; 2) characterize the char; and 3) develop a market for char. The feasibility of using MG chars, alone or as a coal-char blend, in typical industrial pulverized-coal boilers has been examined as one avenue for char use. In the ISGS studies, MG chars of various volatile matter (VM) content have been prepared both in laboratory and pilot plant facilities. In this paper, the effect of char preparation conditions on the physical and chemical properties of MG chars is discussed.

EXPERIMENTAL

Pilot plant-prepared samples - Chars were prepared from sample number 3 of the Illinois Basin Coal Sample Program (IBC-103) (1). This sample is a mine-washed coal (rank HvBb) and consists of a blend of 80% Herrin (No. 6) and 20% Springfield (No. 5) coals. The chars were produced in the Mild Gasification Unit at The United Company (formerly United Coal Company Research Corporation) in Bristol, Virginia (2). The chars were prepared by heating the coal (<2000 μm) under a slight vacuum in an 8-inch i.d., 8-foot fixed-bed reactor. The reactor was located inside a natural gas-fired furnace maintained at 760°C during the production runs. Three partially devolatilized (PD) samples (herein referred to as PD chars) designated as PD-1, PD-2 and PD-3 were prepared using residence times of 1.70, 2.90 and 3.17 hours. For each sample, 38-53, 53-75, 75-105, 105-150 and 150-212 μm particle size fractions were prepared. Further details of sample preparation are given elsewhere (3). All samples were stored under nitrogen prior to use.

Laboratory-prepared samples - Chars were derived from sample number 1 of the Illinois Basin Coal Sample Program (IBC-101). This sample was obtained from the Herrin (Illinois No. 6, HvCb) seam and was a mine-washed coal. Three PD coals (herein referred to as PD-89 chars) were prepared from 150-600 μm IBC-101 coal in a 2-inch i.d. batch fluidized-bed reactor system. A multi-step heating procedure was used to minimize agglomeration of coal particles in the reactor. The final temperature and final soak time were adjusted to produce the desired level of VM in the char. Final temperatures and soak times for laboratory chars were 475°C, 10 mins for the high-volatile char (PD-1-89); 505°C, 30 mins for the medium-volatile char (PD-2-89); and 600°C, 60 mins for the low volatile char (PD-3-89). All samples were ground and sieved in a step wise manner to prepare 38-53, 53-75 and 105-150 μm size fractions. Other details of sample preparation are given elsewhere (4).

Devolatilization behaviors of the coal and chars were determined using a thermogravimetric analyzer (TGA). Each sample was heated in flowing nitrogen (200 cc/min) to 900°C at a constant heating rate of 20°C/min. The weight of sample remaining, the rate of weight loss and the gas temperature in the vicinity of the sample were monitored by a computer as a function of time. The proximate and ultimate analyses and total sulfur contents of the samples were measured using LECO MAC 400, CHN 600, and SC32 analyzers. Internal surface areas of the samples were obtained from nitrogen and carbon dioxide absorption at -196° and -77°C, respectively. Ash

composition and ash fusion temperatures of the samples were determined according to method ASTM D1857.

Reactivities of chars were measured in air using the TGA system. A sample mass of 2-4 mg was heated at 50°C/min under nitrogen flow (200 cc/min) to between 400 and 480°C for these experiments. A modified TGA quartz furnace tube was used to allow the reactant gas (200 cc/min) to enter the quartz reactor tube directly (3). The objective was to achieve, as quickly as possible, a uniform concentration when the reactant gas was introduced into the furnace tube to obtain reliable rate data in the initial stage of reaction. The percent weight of the char remaining, the rate of weight loss and gas temperature in the vicinity of the sample were monitored.

RESULTS AND DISCUSSION

The results of the proximate and ultimate analyses for 105-150 μm IBC-101, IBC-103, PD chars and PD-89 chars are given in table 1. The VM contents (dry basis) of pilot plant chars were 22.1% (PD-1), 14.1% (PD-2) and 10.3% (PD-3). The laboratory chars had VM contents (dry basis) of 18.5% (PD-1-89), 15.4% (PD-2-89) and 9.8% (PD-3-89). Coal IBC-101 has a higher VM and sulfur content, and lower carbon content, than IBC-103. The laboratory chars had projected SO_2 emissions 27% less than IBC-101 while pilot plant chars had projected SO_2 emissions 14% less than IBC-103 coal. The differences in projected emissions could be that only half the sulfur present in IBC-103 is organic sulfur, while nearly 75% of the sulfur in IBC-101 is present in the organic form. It has been shown that at pyrolysis temperatures below 600°C, organic sulfur is more easily removed than pyritic sulfur (5).

The TGA devolatilization profiles of 105-150 μm IBC-103 and pilot plant chars are shown in figure 1. The devolatilization process for coal can be divided into three stages: stage I, below 380°C, the loss of "free" moisture and the release of trapped gases and low molecular weight materials; stage II, 380°C to 550°C, the release of major amounts of tar and gas; and stage III, the thermal decomposition and/or reactions of pyrite impurities in the coal and secondary pyrolysis of the char (6).

Devolatilization profiles obtained for pilot plant chars (figure 1) exhibit weight loss in the three stages described for the coal. The weight loss (about 2.2%) in stage I could have been due to oil and tars that were trapped within the particles during preparation of these chars. TGA analysis to determine boiling point curves for coal oil and tars have indicated that these materials devolatilize below 400°C (7). Weight losses for stage II were about 14% for PD-1, 7.5% for PD-2, and 5% for PD-3. This stage of reaction should be absent for chars that have already been processed at temperatures above 550°C. The weight loss for IBC-103 coal was about 25% between 380 and 550°C. The fact that pilot plant chars lose weight in stage II indicates varying amounts of "coal-like" material remaining in these chars. Devolatilization data for a 15% VM coal-char blend prepared by mixing a char made in a microbalance reactor at 800°C with IBC-103 are shown in figure 1. It is seen that between 350-550°C, the shape of the weight loss curve for the coal-char blend is similar to that of PD-2; confirming the notion that the pilot plant chars contain coal-like material.

Because the pilot plant reactor was heated externally, it is expected that, due to heat transfer limitations, coal particles in the center of the 8-inch reactor were subjected to temperatures lower than those near the wall of the reactor. Unsteady-state one-dimensional heat transfer calculations revealed that the temperature near the center of the reactor was less than 400°C, temperatures at which the rate of pyrolysis is appreciable, even after 3 hours. This implies that there was a radial temperature profile at least within a portion of the reactor. As a result, coal particles were subjected to various thermal histories producing mixtures of highly devolatilized coal and "raw" coal.

The weight percent of coal-like material in each char was calculated using the relationship given below.

$$p = \frac{W_{PD}/(W_{PD} + FC_{PD})}{W_c/(W_c + FC_c)} \times 100\%$$

where: W_c = percent weight loss in stage II for coal; W_{PD} = percent weight loss in stage II for chars; FC_c = percent fixed carbon (dry-ash-free basis) in coal; and FC_{PD} = percent fixed carbon (dry-ash-free basis) in chars. The values of FC_c and FC_{PD} were obtained from table 1. A value of 25.6% was used for W_c (see figure 1). These calculations show that for 105-150 μm chars, the amount of coal-like material present in PD-1, PD-2 and PD-3 was 49%, 24% and 14%, respectively.

The devolatilization profiles of 105-150 μm IBC-101 coal and laboratory chars are shown in figure 2. Coal IBC-101 exhibits a volatile release profile similar to that of IBC-103. The weight loss below 150°C amounted to 6.5% for IBC-101, and less than 1.0% for the laboratory chars. The weight loss between 150 and 380°C was about 2% for the coal, and less than 1% for the laboratory chars. For these chars a noticeable weight loss begins about 460°C for PD-1-89, 520°C for PD-2-89 and 615°C for PD-3-89. These temperatures are consistent with the maximum heat treatment temperatures used during laboratory char preparation. This indicates that laboratory chars were homogeneous and not mixtures of highly devolatilized coal and raw coal.

Internal surface areas for 53-75 μm samples are presented in table 2. The two coals have comparable CO_2 surface areas, but IBC-101 had a substantially higher N_2 surface area than IBC-103. The CO_2 surface areas for the coals ranged from 216 to 239 m^2/g and were typical of HvC bituminous coals. Chars had lower N_2 -BET surface areas than their parent coal, indicating perhaps that the incomplete removal of volatile matter resulted in partial plugging of a large fraction of the pores in the coal that were previously accessible to N_2 at -196°C. The extent of devolatilization had little influence on development of CO_2 surface area. The pilot plant chars had lower CO_2 surface areas than IBC-103, whereas the laboratory chars had higher CO_2 surface areas than IBC-101. The laboratory chars (PD-3-89) had about twice the surface area of the pilot plant chars (PD-3). It has been found previously that chars prepared from IBC-101 and IBC-103 under identical conditions in laboratory-scale reactors had identical surface areas (5). This suggests that different char preparation conditions, not different parent coals, are responsible for differences in surface areas of the chars. During laboratory char preparation, special precautions were taken to minimize agglomeration of IBC-101, while no such precautions were used for pilot plant char production using IBC-103. This could explain the differences in the surface areas of the chars, but without further study, no definite conclusions can be inferred.

Apparent rates [$R = (1/m)dm/dt$; m = mass (ash-free) of sample] from TGA reactivity tests, calculated at 50% burn-off, indicate virtually no dependence on particle size in the temperature range used for oxidation studies (400-480°C) (2,3). This suggests that oxidation rates were sufficiently low such that pore diffusion had no rate-limiting effect and the reaction proceeded under kinetically controlled conditions.

Arrhenius plots (apparent rates vs $1/T$) for PD-3 and PD-3-89 chars are presented in figure 3. The activation energies calculated are approximately 33 kcal/mol for both chars. Laboratory chars are about an order of magnitude more reactive than pilot plant chars. A comparison of reactivities of these chars, with those reported previously for chars prepared from Illinois No. 6 coal (3,8,9), is also shown in figure 3. The reactivity of PD-3-89 (laboratory-prepared char) is comparable with those of chars prepared in similar laboratory-scale reactors (3,8). A 15% VM char prepared in the TGA from IBC-103 (the same coal used to prepare PD-3) exhibited similar reactivity to that of PD-3-89. PD-3 has reactivity comparable to the reactivity which has been reported

for a pilot-scale char (9). These results confirm that char preparation conditions and reactor size and type influence the reactivity of the resultant char.

Ash composition and ash fusion temperature data were used to calculate a number of empirical parameters (10). The results of these tests and other ash characterization data for IBC-101, IBC-103, PD-3 and PD-3-89 are compiled in table 3. The two coals exhibit differences in ash composition which can affect the empirical parameters derived. Coal IBC-101 has a higher concentration of CaO, Na₂O and SO₃, and a lower concentration of Al₂O₃ than IBC-103. The higher Na₂O content translates into a significantly higher fouling index for IBC-101 (high fouling type) than IBC-103 (low fouling type) (10). The slagging index (10) for IBC-101 is significantly higher than that of IBC-103 due to the higher sulfur content of IBC-101. Both coals, however, fall in the range consistent with medium-slagging coals.

A direct comparison of the ash properties of PD-3 and PD-3-89 is not appropriate since the ash properties of the parent coals are different. However, the ash composition and ash characteristic values for PD-3 and PD-3-89 are nearly identical to those of their parent coals. MG processes did not significantly alter the composition of the ash, and there is no evidence that chars have different slagging or fouling indices than those of their parent coals.

SUMMARY AND CONCLUSIONS

Chars with about 10, 15 and 20 percent VM were prepared from Illinois coals under mild gasification conditions both in pilot- and laboratory-scale reactors. The method of char preparation influenced the physical and chemical properties of the chars. Pilot-scale chars were mixtures of highly devolatilized coal and relatively unreacted coal, and had devolatilization characteristics similar to a blend prepared by mixing the parent coal and char. Pilot-scale chars were an order of magnitude less reactive than laboratory-scale chars. Measured CO₂ surface areas of laboratory-scale chars were about two times greater than those of pilot-scale chars. MG processes did not significantly alter the composition of the ash, and there was no evidence that chars have different slagging or fouling indices than their parent coals.

ACKNOWLEDGEMENTS

This work has been sponsored by the Illinois Department of Energy and Natural Resources through its Coal Development Board and Center for Research on Sulfur in Coal.

REFERENCES

1. Harvey, R. D. and C. W. Kruse, 1988. *J. Coal Qual.*, 7(4), pp. 109-112.
2. Rostam-Abadi, M., J. A. DeBarr, C. W. Kruse, D. L. Moran, R. D. Harvey and R. R. Frost, 1987. Final Technical Report, CRSC, Champaign, IL.
3. Rostam-Abadi, M., J. A. DeBarr and W. T. Chen, 1988. "Combustion Characteristics of Coal-derived Solid Fuels". Final Technical Report, CRSC, Champaign, IL.
4. Rostam-Abadi, M., J. A. DeBarr, R. D. Harvey, S. A. Benson, D. P. McCollor, 1989. "Reactivity and Combustion Properties of Coal-derived Solid Fuels". Final Technical Report, CRSC, Champaign, IL.
5. Hackley, K. C., R. R. Frost, C-L. Liu, S.J. Hawk and D. D. Coleman, 1990. *Illinois State Geol. Survey Circ.* #545.
6. Rostam-Abadi, M. and C. W. Kruse, 1983. *Proc. of the 12th Annual North Amer. Thermal Analysis Society Conf.*, paper #175.
7. Kruse, C. W., A. D. Williams and F. D. Guffey, 1989. Final Technical Report, CRSC, Champaign, IL.
8. Khan, M. R., 1987. *Fuel*, 66(12), pp. 1626-1634.
9. Dutta, S. and C. Y. Wen, 1977. *Ind. Eng. Chem. Process Des. Dev.*, 16(1), pp.31-37
10. Attig, R. C. and A. F. Duzy, 1969. *Proc. Amer. Power Conf.*, 31, pp. 290-300.

Table 1. Proximate and ultimate analyses for 105-150 μm fuels (dry basis).

	IBC-101	PD-1-89	PD-2-89	PD-3-89	IBC-103	PD-1	PD-2	PD-3
Moisture	6.6	1.3	1.3	0.6	2.0	2.1	1.9	1.8
<u>Proximate</u>								
Volatile Matter	42.0	18.5	15.4	9.8	36.7	22.1	14.1	10.3
Fixed Carbon	48.4	68.4	71.8	76.6	54.3	67.5	74.2	78.0
<u>Ultimate</u>								
Hydrogen	5.04	3.47	3.08	2.16	5.13	3.47	2.39	1.64
Carbon	69.68	72.55	75.66	77.99	75.06	77.85	79.71	80.58
Nitrogen	1.44	1.70	1.82	1.87	1.67	1.95	1.92	1.78
Oxygen	9.96	5.83	3.74	1.48	6.89	4.43	2.46	2.46
Sulfur	4.28	3.35	2.96	2.93	2.24	1.95	1.81	1.79
Ash	9.6	13.1	12.7	13.6	9.01	10.34	11.71	11.74
Btu/lb	12790	12504	12716	12706	13490	13245	13010	12828
lbs SO ₂ /MM Btu	6.7	5.4	4.7	4.6	3.3	2.9	2.8	2.8

Table 2. Surface areas for 53-75 μm fuels.

	IBC-101	PD-1-89	PD-2-89	PD-3-89	IBC-103	PD-1	PD-2	PD-3
BET(CO ₂)	239	249	305	354	216	194	175	165
BET(N ₂)	61.3	2.0	3.8	9.5	3.8	1.2	1.0	0.8

Table 3. Ash characterization of coals and chars.

Character	IBC-101	PD-3-89	IBC-103	PD-3
<u>Ash analyses (% of ash)</u>				
SiO ₂	48.60	48.20	49.63	47.77
Al ₂ O ₃	17.49	17.36	22.13	21.82
Fe ₂ O ₃	18.22	18.08	18.16	21.82
CaO	4.89	4.76	1.59	1.58
MgO	0.99	0.98	0.92	0.90
K ₂ O	2.22	2.22	2.44	2.35
Na ₂ O	1.47	1.50	0.33	0.30
TiO ₂	0.89	0.90	1.30	1.20
P ₂ O ₅	0.27	0.26	0.33	0.37
MnO	0.05	0.06	0.02	0.03
SrO	0.04	0.04	0.06	0.03
BaO	0.04	0.04	0.06	0.05
SO ₃	4.19	4.29	1.43	1.22
Silica ratio	68.85	66.93	70.6	69.0
Base/acid	0.41	0.41	0.32	0.34
<u>Ash fusion temp., °F, reducing</u>				
Initial deformation	2055	2115	2000	2050
Softening	2140	2185	2160	2220
Hemispheric	2225	2260	2310	2335
Fluid	2310	2330	2465	2460
<u>Empirical ash properties</u>				
T ₂₅₀ , °F	2425	2460	2490	2510
T _{cv} , °F	2584	2584	2305	2310
Slag viscosity (poise @2600°F)	105	106	175	140
Slagging				
index	1.75	1.20	0.71	0.61
type	medium	medium	medium	medium
Fouling				
index	0.60	0.62	0.11	0.11
type	high	high	low	low

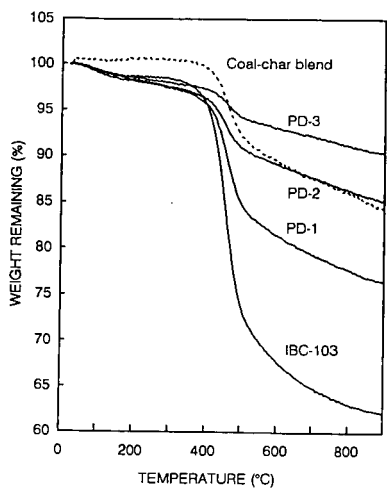


Figure 1. TGA devolatilization profiles for IBC-103, PD chars and a coal-char blend.

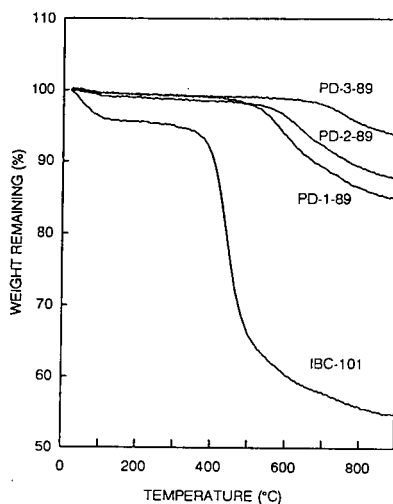


Figure 2. TGA devolatilization profiles for IBC-101 and PD-89 chars.

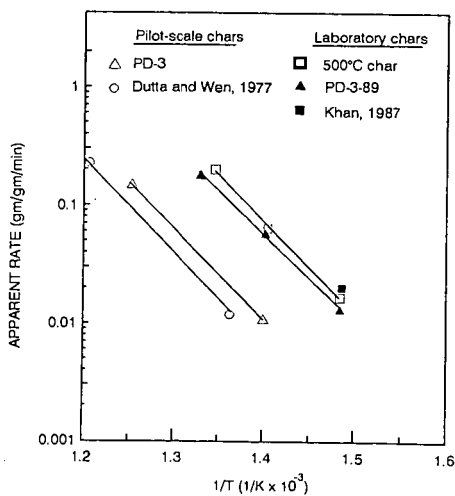


Figure 3. Arrhenius plot for fuels in 1 atm air

PREDICTING THE TRANSIENT DEVOLATILIZATION OF VARIOUS COALS WITH FLASHCHAIN

Stephen Niksa
High Temperature Gasdynamics Laboratory
Mechanical Engineering Department
Stanford University, Stanford, CA 94305

Alan R. Kerstein
Combustion Research Facility
Sandia National Laboratories
Livermore, CA 94550

Keywords: Modeling; Coal Rank Effects; Transient Devolatilization

INTRODUCTION

In coal-fired utility boilers, devolatilization generates the gaseous fuel compounds which ignite and stabilize the flame. Precursors to noxious gases are also released as the coal thermally decomposes. Pulverized coal injected into hot gases devolatilizes while it heats at $10^4 - 10^5$ K/s. The process takes only several milliseconds, and is completed before the fuel reaches its ultimate temperature. The rank of coal largely determines the total amount of volatiles as well as the proportions of heavy aromatic tar compounds and noncondensable gases. Coal rank is also an influence on the reaction rate, albeit a poorly characterized one. Until very recently no reliable transient data were available for boiler conditions, although laboratory studies at slower heating rates indicated that low rank coals devolatilize significantly faster than bituminous coals.¹

This study uses FLASHCHAIN²⁻⁴ to demonstrate that continuous variations of only a handful of structural features in the coal and one rate constant underlie the transient devolatilization of coals across the rank spectrum. It shows that the ultimate analysis is the only sample-specific data needed for accurate predictions of ultimate tar and total yields with this theory, consistent with a previous parametric sensitivity study.⁴ Lignites and low volatility coals are featured in this evaluation, to complement the emphasis on subbituminous and high volatile (hv) bituminous samples in the first evaluation.⁴ This study extends earlier work further by identifying the parametric basis for reliable transient predictions for rapid atmospheric devolatilization of any coal type.

GUIDELINES FOR THE DATA CORRELATIONS AND MODEL PARAMETERS

Taken together, the two laboratory studies⁵⁻⁶ selected for the model evaluation depict the behavior throughout the entire range of coal types, for wide ranges of temperature and heating rate at atmospheric pressure. Freihaut and Proscia used a wire-grid heater in which the sample was dispersed in a layer only a few particles deep, and assigned process temperatures after very extensively characterizing the vagaries of fine-wire thermocouples in such systems.⁷ Their ultimate weight loss values and tar yields are based on heatup at 725 K/s, followed by 10s at the stated reaction temperatures. Transient weight loss is available for a heating rate of 800 K/s. Even though forced quenching was not implemented, their samples cooled at rates from 1500 to 2000 K/s, which is fast enough to virtually eliminate decomposition during cooling. However, their transient tar yields are too scattered to be used for model evaluations.

Chen and Niksa⁷ used a novel radiant coal flow reactor to impart heating rates exceeding 10^4 K/s. Their calculated thermal histories, described elsewhere,⁸ indicate a nominal heating rate of 15,000 K/s for the long-residence-time-cases considered here. The corresponding model predictions are based on transient heatup at this rate to 1300 K. Predicted tar yields are compared to the sum of the measured yields of tars and oils, consistent with the product recovery scheme in their study.

Collectively 14 different coal samples are represented. As seen in Table I, they represent nominal ranks from lignite to anthracite, and 40% of them are low volatility samples. Note also that in three cases, virtually identical samples were used in both laboratory studies. The atomic H/C and O/C ratios are based on the reported ultimate analyses. The additional structural and characterization data in Table I are needed to define FLASHCHAIN's input parameters. All values are based on regressions of literature values reported elsewhere.^{2,4} So the only coal-specific input for these simulations is the ultimate analyses. Thus, this study will determine if samples having the same nominal rank but different O/C and H/C ratios can be distinguished with this theory, as suggested by a previous study of parametric sensitivity.⁴

All parameters in the constitution submodel are collected in Table II. Four are based on molecular weights: that of the aromatic nucleus, MW_A , is used to normalize those of labile bridges (MW_B/MW_A), char links (MW_C/MW_A), and peripheral groups (MW_P/MW_A). The tabulated values show that nuclei become more massive in coals of higher rank, and both the labile and refractory connections among them become smaller. The proportion of intact links in the whole coal, $p(0)$, follows the tendency in the pyridine extract yields (in Table I) to remain constant for ranks through hv bituminous. It then rises precipitously for coals of higher ranks, consistent with their smaller extract yields because structures which are more tightly interconnected have fewer smaller fragments to be extracted. The fraction of labile bridges among intact links, $F^b(0)$, decreases from its value of unity for lignites in proportion to the carbon content. The values in Table II for carbon contents below 85% are based on the regression reported previously.⁴ However, the sample population for that regression had few low volatility samples, whose total and tar yields were badly scattered. Based on the yields for the 4 samples in Chen and Niksa's study, the last 6 entries in Table II are given by $F^b(0) = 0.096 - 0.031(\%C, \text{daf})$. In the future, this regression will be used for all carbon contents over 86%.

The selectivity coefficient between scission and spontaneous char condensation, v_B , also varies with rank. Since crosslink formation has been clearly related to CO_2 evolution,⁹ the values of v_B are proportional to O/C ratios, but only for values below 0.2 or for carbon contents less than 83%. The latter restriction is consistent with the fact that precursors to CO_2 are either carboxylic acid or ketone functionalities, which are present only in coals having lower carbon contents. The former restriction is based on data correlations for the low carbon-content samples in this study. (Our previous evaluation included no coals with such low carbon contents.)

Regarding the reaction rate parameters, those for recombination and peripheral group elimination and the expression for the saturated vapor pressure of tar precursors, P^{SAT} , are identical to values reported previously, and fixed for all coal types. The mean activation energy for bridge decomposition is also at its former value. But the frequency factor, A_B , and std. dev. in the bridge energy rate, σ , have been generalized in correlations with the carbon content, based on the correlations of transient weight loss presented below. Whereas these parameter correlations assign the same values reported previously for hv bituminous coals,³ they prescribe significantly faster reaction rates at low temperatures for coals of lower rank. However, for ranks above hv bituminous, the bridge decomposition rates vary very little.

In the simulations reported below, the operating conditions of temperature, heating rate, and/or time were varied to match those in the experiments, while all coal properties and rate constants were specified according to Table II. A simulation of each thermal history requires from 2 to 5 minutes on a 386 personal microcomputer operating at 20 MHz, with an 8-Bit Fortran compiler.

RESULTS

Figures 1 and 2 present comparisons among the predicted and measured values of ultimate weight loss and tar yields, respectively. The measurements at 725K/s were taken for a 10 s reaction period at temperatures from 900 to 1100K. Simulations are based on the same heating rate and 5 s at 1000K, which is long enough to simulate complete devolatilization. The predictions are within experimental uncertainty for coals across the rank spectrum, except for the 1520 lignite and the 1516 low volatile bituminous. The latter discrepancy is especially difficult to rationalize because the prediction for 15,000 K/s with a virtually identical sample in Chen and Niksa's data is nearly exact.

Similarly, the significant enhancements in weight loss due to the 20-fold increase in heating rate in this data set are predicted within experimental uncertainty for all coal types.

Predicted tar yields in Fig. 2 are also quantitatively accurate, and there are no systematic deviations with coal rank. FLASHCHAIN also predicts that tar yields are substantially enhanced with faster heating, in accord with the observed behavior of all bituminous samples. Considering that 70% of the predictions in Figs. 1 and 2 (denoted by circles) are based on the parameters identified with an independent data base, these results also demonstrate that the ultimate analysis is the only coal-specific input required for accurate ultimate yields with FLASHCHAIN. The additional data on low volatility samples and the extended correlation for $F^*(0)$ appear to expand the range of rank which can be accurately simulated.

In addition to transient weight loss, this model accurately predicts the temperature dependence of ultimate yields, as seen in Figs. 3 and 4. Simulated transient weight loss is based on heatup at 800 K/s, whereas ultimate yields are based on heatup at 725 K/s, followed by 10 s isothermal reaction periods at the indicated temperatures. In Fig. 3 for the lignite (1443), these three quantities are correlated within experimental uncertainty at all temperatures. In Fig. 4, ultimate weight loss for an hvA bituminous sample (1499) is reliably correlated, but calculated tar yields are high by 4 wt%. Data from this coal also validates the calculated transient weight loss through 1000K. Unfortunately, the current data base can only be used to evaluate transient predictions for ranks through hv bituminous.

DISCUSSION

Predicting the ultimate weight loss and tar yields from any coal type is treated here as a matter of distinguishing aliphatic, heteroatomic, and aromatic constituents, rendering functional groups superfluous. In its submodel for coal constitution, FLASHCHAIN introduces the segregation of all oxygen and aliphatics into labile bridges and peripheral groups, and all aromatics and nitrogen into char links and aromatic nuclei. This crucial partitioning is implemented with balances based on the ultimate analysis, carbon aromaticity, and aromatic carbon number per monomeric unit. (Proton aromaticity is also included but found to be inconsequential.) The predictions reported here demonstrate that the ultimate analysis is the only coal-specific input needed with this theory. Regression values of all other inputs are the basis for accurate predictions, for reasons identified in our previous sensitivity study.⁴ Now that the population for these regressions has been expanded by the addition of a few lignites and several low volatility coals, predictions can be generated for virtually any coal sample. This extension paves the way for examinations of extensive literature data for coal rank effects, now underway.

Regarding transient behavior, FLASHCHAIN reveals a new basis for interpreting and understanding the factors underlying the transient devolatilization of any coal type. FLASHCHAIN now incorporates this tendency through newly-identified correlations of the frequency factor and variance in the energy distribution for bridge decomposition with carbon content. From a practical standpoint, this approach yields reliable predictions for ranks from lignites through hv bituminous, but extensions to low volatility samples must await additional transient data.

From a mechanistic standpoint, inferences based on the trends in these rate constants should be closely circumscribed. Neither FLASHCHAIN nor any other current model includes the types of reaction mechanisms which can associate specific functionalities and reaction channels with the observed tendencies. There is, nevertheless, one obvious implication. In so far as oxygen content diminishes with increasing coal rank, the variations suggest that oxygenated species accelerate reaction rates during the early stages, as expected for any free-radical chain mechanism among hydrocarbons. Indeed, CO_2 and H_2O are major products during the initial stages.⁵ Oxygenated species are also implicated in the broadening of the temperature range for devolatilization with decreasing rank, in that CO is always a major product of the latest stages of devolatilization.⁶

ACKNOWLEDGEMENT

Partial support for S. Niksa was provided by EPRI through their Exploratory Research Program. Partial support for A. R. Kerstein was provided by the Division of Engineering and Geosciences, Office of Basic Energy Sciences., U. S. Department of Energy.

REFERENCES

- Howard, J. B., in *Chemistry of Coal Utilization*, 2nd Suppl. Vol.; Elliot, M.A., Ed.; Wiley-Interscience: New York, 1981; Chapter 12.
- Niksa, S. and Kerstein, A. R., *Energy Fuels* 5(5): 647-664 (1991).
- Niksa, S., *Energy Fuels* 5(5): 665-672 (1991).
- Niksa, S., *Energy Fuels* 5(5): 673-683 (1991).
- Freihaut, J. D. and Proscia, W. M., Final Report to U. S. DOE/Pittsburgh Energy Technology Center for Contract No. DE-AC22-89PC89759, August 1991.
- Chen, J. and Niksa, S., "Coal Devolatilization During Rapid Transient Heating. Part 1: Primary Devolatilization," *Energy Fuels*, to appear, 1992.
- Freihaut, J. D., Proscia, W. M., and Seery, D. J., *Energy & Fuels* 3:692 (1989).
- Chen, J. and Niksa, S., "A Radiant Flow Reactor for High-Temperature Reactivity Studies of Pulverized Solids," *Rev. Sci. Instrum.*, to appear, 1992.
- Suuberg, E. M, Lee, D., and Larsen, J. W., *Fuel* 64:1668 (1985).

Table I. Coal Properties

Sample	%C, daf	H/C	(O+S)/C	f_a'	AC/CI	MW _{MON}	Y _{PYR}	MW _G
1443	66.5	.931	.306	.493	9.7	356	26	26.5
1520	69.0	.877	.271	.533	10.6	348	26	26.5
1488C	69.5	.863	.260	.541	10.8	345	26	26.5
1493C	74.1	.858	.136	.614	12.5	329	26	26.3
1493	75.5	.798	.179	.637	13.1	326	26	25.6
1499	79.9	.825	.122	.706	14.7	312	26	23.7
1451C	82.5	.815	.077	.748	15.7	305	26	22.5
1451	84.0	.803	.079	.772	16.2	300	26	21.8
1516	87.4	.614	.055	.826	17.5	291	26	20.3
CBMC	87.5	.759	.021	.827	17.5	290	26	20.2
1516C	88.7	.676	.018	.846	18.0	288	21.6	19.7
1521C	89.6	.643	.019	.861	18.3	285	14.8	19.3
1508C	89.9	.614	.035	.865	18.4	284	12.5	19.2
1468	94.3	.237	.024	.935	20.1	276	0	17.2

*The suffix "C" denotes samples of Chen and Niksa;⁶ all others are Freihaut and Proscia's.⁵

Table II. Structural Model Parameters

Sample	MW _A	C _A	MW _B /MW _A	MW _C /MW _A	MW _G /MW _A	p(0)	F ^B (0)	v _B	v _E
1443	125	9.7	1.859	.836	.511	.911	1.000	.150	2.40
1520	134	10.6	1.602	.721	.442	.911	1.000	.150	2.23
1488C	135	10.7	1.563	.704	.430	.911	0.983	.150	2.19
1493C	148	11.6	1.307	.588	.359	.911	0.858	.329	2.03
1493	152	11.9	1.258	.566	.347	.911	0.821	.202	2.05
1499	165	12.9	1.044	.470	.288	.911	0.702	.370	2.00
1451C	176	13.7	0.901	.406	.247	.911	0.632	.500	1.93
1451	180	14.1	0.838	.377	.230	.911	0.591	.500	1.90
1516	169	13.4	1.079	.485	.297	.911	0.329	.500	2.48
CBMC	182	14.2	0.886	.399	.243	.911	0.366	.500	2.19
1516C	183	14.4	0.866	.390	.239	.920	0.329	.500	2.21
1521	186	14.6	0.836	.376	.230	.937	0.301	.500	2.21
1508C	181	14.4	0.897	.404	.247	.943	0.291	.500	2.33
1468	178	14.5	1.005	.452	.097	1.000	0.154	.500	2.86

Evaluation of Predicted Ultimate Weight Loss

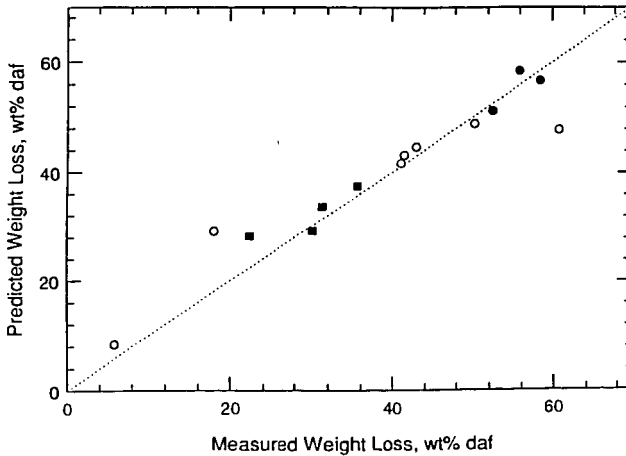


Figure 1. An evaluation of predicted weight loss for the coals in Table I versus measured values. Measured values were reported by Freihaut and Proscia² for atmospheric devolatilization for a heating rate of 725 K/s and 10 s at temperatures from 900 to 1100 K (open symbols); and by Chen and Niksa³ for a heating rate of 15,000 K/s to a temperature high enough to achieve complete primary devolatilization (filled symbols). Predicted values are based on the parameters in Tables II and III and heatup at 725 K/s with 5 s at 1100 K and at 15000 K/s to 1300K. All cases denoted by circles are based solely on parameter values assigned for an independent data base.

Evaluation of Predicted Ultimate Tar Yields

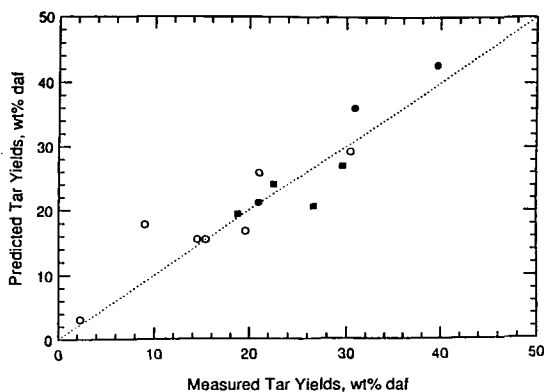


Figure 2. An evaluation of predicted ultimate tar yields for the coals in Table I versus measured values. Measured values were reported by Freihaut and Proscia⁵ for atmospheric devolatilization for a heating rate of 725 K/s and 10 s at temperatures from 900 to 1100 K (open symbols); and by Chen and Niksa⁶ for a heating rate of 15,000 K/s to a temperature high enough to achieve complete primary devolatilization (filled symbols). Predicted values are based on the parameters in Tables II and III and heatup at 725 K/s with 5 s at 1100 K and at 15000 K/s to 1300K. All cases denoted by circles are based solely on parameter values assigned for an independent data base.

Transient and Ultimate Yields for 1443

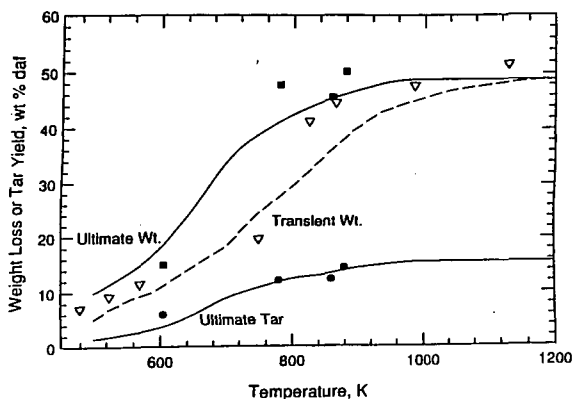


Figure 3. Comparisons between measured and predicted ultimate weight loss and tar yields and weight loss during transient heatup for a lignite (1443). Data were reported by Freihaut and Proscia⁵ for a heating rate of 725 K/s and 10 s at the indicated temperatures, for ultimate values, and rates from 650 to 1250 K/s and nominal cooling rates from 1500 to 2000 K/s for the transient data. The respective simulations are based on identical conditions for the ultimate yields, and a heating rate of 800 K/s to the indicated temperatures without allowing for decomposition during cooling, which is negligible at such fast cooling rates.

Transient and Ultimate Yields for 1499

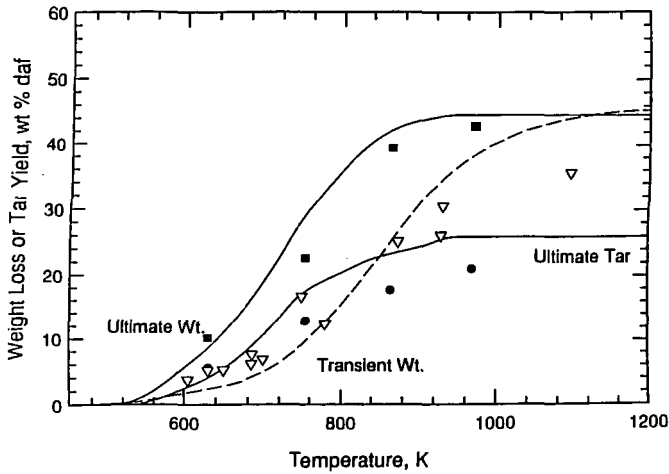


Figure 4. Comparisons between measured and predicted ultimate weight loss and tar yields and weight loss during transient heatup for an hvA bituminous coal (1443). Data were reported by Freihaut and Proscia⁵ for a heating rate of 725 K/s and 10 s at the indicated temperatures, for ultimate values, and rates from 650 to 1250 K/s and nominal cooling rates from 1500 to 2000 K/s for the transient data. The respective simulations are based on identical conditions for the ultimate yields, and a heating rate of 800 K/s to the indicated temperatures without allowing for decomposition during cooling, which is negligible at such fast cooling rates.

IMPROVED DIFFERENTIATION OF SULFUR FORMS IN COALS BY
SELECTIVE DEGRADATION WITH PERCHLORIC ACID MIXTURES

R. Markuszewski^a, X. Zhou, and C. D. Chriswell
Fossil Energy Program, Ames Laboratory, Iowa State University
Ames, Iowa 50011

and

^aInstitute of Gas Technology, Chicago, IL 60616

Keywords: sulfur forms in coal; coal analysis for sulfur;
perchloric acid dissolution of coal

INTRODUCTION

Recent work at the Ames Laboratory has resulted in proposing a promising new technique for determining sulfur forms in coal based upon the step-wise oxidation of coal with perchloric acid (1). Initial results on determination of sulfur forms by selective oxidation with perchloric acid have been very encouraging (2). Relatively sharp and reproducible delineations have been observed for sulfide, sulfate, pyritic, and organic sulfur in some cases. Other preliminary studies on model organosulfur compounds have shown it to be possible to differentiate between at least two groups of organic sulfur compounds by this technique (3). In more recent work, the reproducibility of these results has been confirmed, more detailed conditions for extracting selectively the various sulfur species have been specified, and more coal samples with higher organic sulfur content have been tested.

EXPERIMENTAL PROCEDURES

Based upon earlier observations of the behavior of coal, pyrite, and sulfate salts with boiling HClO_4 at various temperatures (1), a reaction scheme was developed for the direct determination of sulfur forms in coal which uses the variable oxidizing power of HClO_4 to dissolve selectively sulfur-containing components and convert them to sulfate for turbidimetric measurement. In the original procedure for the consecutive determination of sulfur forms in a single sample of coal (2), sulfate was extracted with a HClO_4 solution boiling at 120°C, pyrite with a HClO_4 solution boiling at 155°C, and organic sulfur with a solution of 9:1 HClO_4 - H_3PO_4 boiling at 205°C. In all 3 steps, sulfur-containing gases were trapped in 15% H_2O_2 , and sulfate was determined in the trap and in the aqueous filtrate. If any sulfide was present, it was captured and measured in the H_2O_2 -filled gas trap during the extraction of sulfate. For some coals, however, total sulfur recovered was slightly less than total sulfur in the coal (0.2-0.4% abs.). The low recovery could be due to: 1) incomplete absorption of sulfur-containing gases by the neutral H_2O_2 solution in the trap, 2) dissolution of some organosulfur compounds at 155°C without total conversion to sulfate, and 3) analytical factors, such as incomplete precipitation of BaSO_4 due to high acidity. For other coal samples, the discrepancy between pyritic and organic sulfur forms determined by the ASTM and the HClO_4 procedures was significant. Some of these possibilities have been tested experimentally in previous work (4-6).

RESULTS AND DISCUSSION

Determination of Sulfur Forms in Coal

Using the original procedure, the following results were obtained for sulfur forms in Illinois, Pittsburgh, and New Zealand coals (minus 60 mesh) and in another Illinois No. 6 coal (minus 200 mesh), as shown in Table 1. While for the minus 60-mesh coal samples the agreement between the HClO_4 and ASTM procedures for pyritic and organic sulfur forms is reasonable, it is quite divergent for the minus 200-mesh sample. Therefore, further tests were conducted to test the conditions for selective extraction of sulfur forms.

Table 1. Sulfur Form (in %) Determined by HClO_4 and ASTM Procedures

	Sulfate	Sulfide	Pyritic	Organic	Total
<u>Illinois No. 6 (-60 mesh)</u>					
HClO_4 (avg. of 4 detns.)	0.74	0.02	1.79	1.64	4.19
ASTM (1 detn.)	0.75	n.d.	1.69	1.77	4.21
<u>Pittsburgh No. 8 (-60 mesh)</u>					
HClO_4 (avg. of 2 detns.)	0.48	0.01	1.13	1.32	2.94
ASTM (1 detn.)	0.49	n.d.	1.18	1.47	3.14
<u>Charming Creek N.Z. (-60 mesh)</u>					
HClO_4 (1 detn.)	0.04	0.01	0.11	5.02	5.18
ASTM (1 detn.)	0.04	n.d.	0.02	5.38	5.44
<u>Illinois No. 6 (-200 mesh)</u>					
HClO_4 (avg. of 2 detns.)	0.24	0.04	3.27	1.38	4.93
ASTM (1 detn.)	0.20	n.d.	2.87	1.85	4.92

Dissolution of Sulfur from Coal as a Function of Temperature

The original procedure, based on extracting -60 mesh coal using the boiling point of the pure HClO_4 solution as the temperature guide, resulted in typical S-shaped dissolution curves, as shown previously (1) for an Illinois No. 6 coal sample containing 4.85% total sulfur (0.26% sulfate, 2.42% pyritic, and 2.17% organic sulfur). Although there was a lot of scatter for that -60 mesh coal, it was on the basis of such curves, as well as the behavior of pure pyrite and mineral sulfate, that the HClO_4 b.p. of 120, 155, and 203°C were selected for the extraction of sulfate, pyritic, and organic sulfur, respectively.

When the extraction procedure was repeated for another Illinois No. 6 coal, -200 mesh and containing 4.98% total sulfur (0.04% sulfate, 3.04% pyritic, and 1.90% organic sulfur), the much smoother curve depicted in Figure 1 was obtained. In this and all subsequent figures, the temperature of the reaction mixture (HClO_4 plus coal) is plotted. The curve shows a definite break at ~140-145°C, showing a clear delineation between pyritic and organic sulfur.

Analysis of Coal Residues After HClO_4 Extraction

In order to get additional information about the possible dissolution of organic sulfur and the oxidation of organic matter in the coal, the undissolved materials from HClO_4 extractions at several temperatures, as well as a sample of the raw coal, have been further analyzed for organically associated S, Cl, and O using our SEM-EDX procedure described earlier (7).

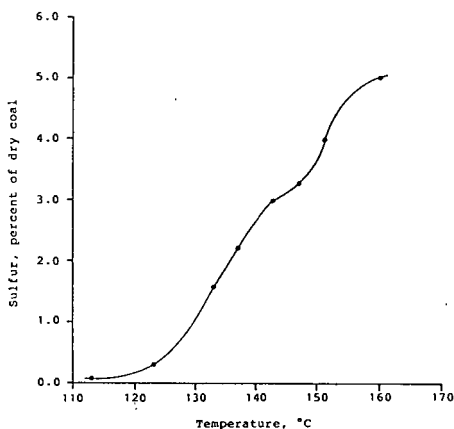


Figure 1. Total sulfur recovered (as percent of dry coal) as a function of reaction temperature for Illinois No. 6 coal (~200 mesh)

Because this technique measures organically bound elements on a dry, mineral matter-free (dmmf) basis, the results could not be directly compared to those obtained by the ASTM or HClO_4 procedures (the coal contained 28.8% ash). However, there were several interesting trends. First of all, it was evident that the organic sulfur content was fairly constant, within the experimental errors of this technique, until a temperature of about 147°C. At the same time, there was a significant increase in organic oxygen and chlorine as the temperature increased. This was not unexpected since the coal was being oxidized, and chlorination is known to occur during the perchloric acid degradation of organic compounds (3). When corrected for O and Cl content, the organic S content appeared to be fairly constant almost up to 151°C.

Dissolution of Iron During Extraction of Sulfur from Coal

The solutions from Illinois coal samples extracted for sulfur at different temperatures (Figure 1) were also analyzed for iron by atomic absorption spectrophotometry. The results are presented in Figure 2, and the amount of undissolved material is presented in Figure 3. It is evident that the amount of dissolved iron increases up to ~143°C and then becomes constant, indicating that all the pyrite has been dissolved before the coal matrix starts to be dissolved. Also, at 113°C, where only sulfate is extracted, pyrite is not dissolved.

Dissolution of Coal During Extraction of Sulfur

Figure 3 represents the weight loss for the same Illinois coal sample depicted in Figure 1. It is evident that the amount of undissolved material does not decrease until temperatures of ~143°C are reached, indicating that the organic matrix and the associated organic sulfur have not been leached out at a temperature at which pyrite has been dissolved. This is also corroborated by the color of the extracts, which are colorless or pale yellow until ~143°C

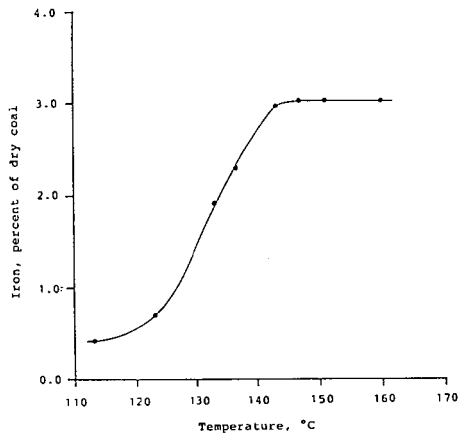


Figure 2. Dissolved iron (as percent of dry coal) as a function of reaction temperature for Illinois No. 6 coal (-200 mesh)

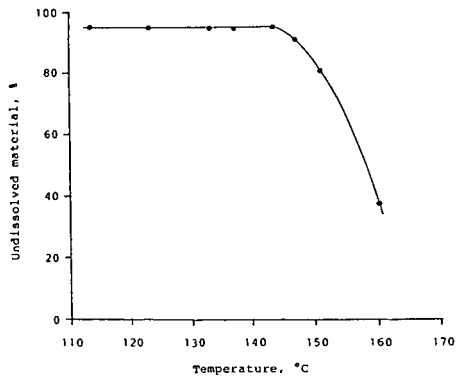


Figure 3. Undissolved material as a function of reaction temperature for Illinois No. 6 coal (-200 mesh)

and then become orange to deep-brown at higher temperatures at which coal begins to dissolve. Further details of these observations are described elsewhere (8).

New Procedure for Determination of Sulfur Forms

Based upon the results above, it was concluded that better delineation of sulfur forms could be obtained by employing lower temperatures for the dissolution steps, i.e., 110°C for sulfate and 143°C for pyrite sulfur. Applying this modified procedure to another sample of Illinois No. 6 coal gave the results presented in Table 2. It is evident that the agreement between these results and those from ASTM procedures is very good.

Table 2. Sulfur forms (percent of dry coal) in Illinois No. 6 (bottle 7) by HClO₄ procedure using new step-wise oxidation conditions.

S form	Mixture Temp. (°C)	% S (dry basis)				% S by ASTM (dry basis)
		Expt.1	Expt.2 ^a	Expt.3 ^a	Average	
Sulfate	110	0.07	0.07	0.07	0.07	0.04
Pyritic	143	2.99	2.91	2.98	2.96	3.04
Organic	180-200	1.71	1.79	1.76	1.75	1.88
Totals		4.77	4.77	4.81	4.78	4.96

^aHClO₄-H₃PO₄(9:1) mixture.

Dissolution of Coal in HClO₄ With Admixtures

In order to obtain even more selectivity, several admixtures were tested with HClO₄ to alter its oxidizing power. One was the addition of H₃PO₄ to promote the dissolution of pyrite and thus extract all pyritic sulfur at a lower temperature without affecting the organic sulfur. In practice, the results were not useful. While the temperature of dissolution was lowered by a few degrees, no further enhancement of differentiation was observed.

The addition of iron salts, however, was more useful. It was anticipated the ferric salts would promote the dissolution of pyrite, as demonstrated by the Meyers process. Catalytic amounts (50-100 mg) of FeCl₃ or Fe(ClO₄)₃ showed no activity. But when a series of extractions was performed at a lower temperature, at which it is known that HClO₄ by itself does not extract all the pyrite, with increasing amounts of Fe(ClO₄)₃ added to the mixture and boiled for 1.5 or 2.5 h, the curve depicted in Figure 4 was obtained.

For the extraction of coal with varying amounts of added Fe(ClO₄)₃ for 1.5 or 2.5 h at 134.5°C, the amount of S removed increased rapidly from 0 to 0.05M Fe(ClO₄)₃. From 0.05 to 0.7M Fe(ClO₄)₃, the amount of S removed continued to increase less rapidly, and above 0.7M Fe(ClO₄)₃ it was fairly constant. These data imply that all the inorganic S could be removed at 134.5°C in the presence of as little as 0.05M Fe(ClO₄)₃, compared to 143°C required in its absence. They also imply that some organic S form (~0.9%) is labile and can be removed in the presence of <0.7M Fe(ClO₄)₃ at a temperature of only 134.5°C.

Dissolution of Coals With High Organic Sulfur in HClO₄

For a Spanish lignite (9.63% tot. S, 0.05% sulf. S, 1.06% pyr. S, and 8.52% org. S, as determined by ASTM), a break occurred at ~140°C, corresponding to ~2.5% S; this compares with 1.1% inorganic S by ASTM. Thus, it is very likely that

~1.4% additional (and therefore "organic" sulfur) was dissolved at this temperature. The form of this "organic" sulfur is unknown; it could be noncarbon-bonded sulfur. But the fact is that some form of sulfur that is classified as organic sulfur by ASTM dissolved under these mild conditions. Another break occurred at about 160-167°C corresponding to about 6-7% S, and the remainder of the sulfur dissolved at about 200°C. This would imply that the lignite might contain about 1.1% inorganic S, 1.4% very easily oxidized "organic" S, about 3.5-4.5% organic S that is comparable to that in Illinois No. 6 coal, and about 3-4% organic S which is more difficult to remove. For a specially prepared Bevier seam coal (containing ~3% total S of which ~2.5% is organic S), the results are less easily interpreted. Additional experiments are being carried out to characterize the S forms in more detail.

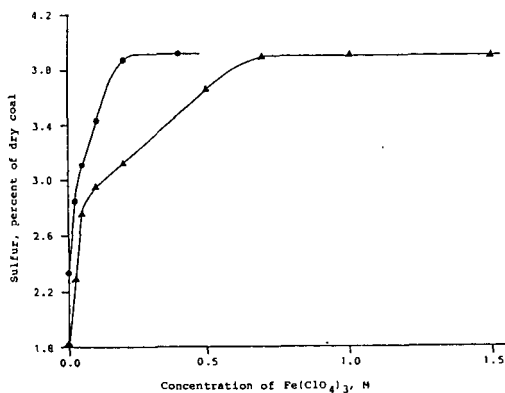


Figure 4. Total sulfur recovered (as percent of dry Illinois No. 6 coal) as a function of $\text{Fe}(\text{ClO}_4)_3$ concentration at 134.5°C

▲ extraction time 1.5 h; ● extraction time 2.5 h

CONCLUSIONS

The delineation of S forms in coal is possible by selective oxidative degradation with boiling HClO_4 . In the plot of total sulfur extracted by boiling HClO_4 of various concentrations, there is a clear delineation between sulfate and pyritic S and between pyritic and organic S. The temperatures at which such differentiations can be made are somewhat lower than previously expected and thus provide better conditions for a more accurate measurement of the various S forms in coal.

The extraction of pyritic S is also directly related to the amount of extracted iron. Organic S is extracted only when oxidative degradation of coal becomes significant, signalling the dissolution of coal, as shown by the deepening color of the extracts and the analyses of the residues.

The presence of $\text{Fe}(\text{ClO}_4)_3$ enhanced the selectivity of HClO_4 in the extraction of sulfur from coal, especially at lower temperatures. Increasing the

$\text{Fe}(\text{ClO}_4)_3$ concentration up to 0.05M allowed the removal of all inorganic sulfur at 134.5°C. Increasing the $\text{Fe}(\text{ClO}_4)_3$ concentration further, up to 0.7M but still at 134.5°C, removed a significant portion of what has to be labile organic S. Further increases in $\text{Fe}(\text{ClO}_4)_3$ concentration did not remove additional organic S. This has to be termed intractable organic S and could be related to the thiophenic-type S.

The HClO_4 dissolution procedure applied to a Spanish lignite with high organic S, showed 4 different forms of S. But specific assignment of functionality to all 4 classes is not as yet possible. Further tests are continuing on this Spanish lignite and on Bevier coal, both containing mostly organic S.

ACKNOWLEDGEMENT

The experimental work was done at Ames Laboratory which is operated for the Department of Energy by Iowa State University under Contract No. W-7405-Eng-82. Most of this work was supported by the Assistant Secretary for Fossil Energy, through the Pittsburgh Energy Technology Center.

REFERENCES

1. C. W. McGowan and R. Markuszewski, "Fate of Sulfur Compounds in Coal During Oxidative Dissolution in Perchloric Acid," Fuel Processing Technology, 17(1), 29-41 (1987).
2. C. W. McGowan and R. Markuszewski, "Direct Determination of Sulfate, Sulfide, Pyritic, and Organic Sulfur in a Single Sample of Coal by Selective, Step-Wise Oxidation with Perchloric Acid," Fuel, 67(8), 1091-1095 (1988).
3. C. W. McGowan, K. Qualls Cates, and R. Markuszewski, "The Conversion of Organic Sulfur in Coal to Sulfate Using Perchloric Acid," Am. Chem. Soc. Div. Fuel Chem. Preprints, 33(1), 225-231 (1988).
4. K. S. Ailey Trent, C. W. McGowan, and R. Markuszewski, "Analysis for Organosulfur Compounds in Perchloric Acid Solutions Resulting from the Oxidation of Coal for the Determination of Pyrite," presented at ACS meeting, Atlanta, GA, April 14-19, 1991.
5. X. Zhou and R. Markuszewski, "Characterization of Sulfur Forms in Coal by Oxidative Degradation," presented at Iowa Academy of Science Annual Meeting, Dubuque, IA, April 19-20, 1991.
6. K. S. Ailey Trent, C. W. McGowan, E. Lachowicz, and R. Markuszewski, "A Standard Addition Method for the Measurement of Sulfate Produced During the Determination of Sulfur Forms in Coal Using Perchloric Acid," Am. Chem. Soc. Div. Fuel Chem. Preprints, 36(3), 1198-1203 (1991).
7. W. E. Straszheim, R. T. Greer, and R. Markuszewski, "Direct Determination of Organic Sulphur in Raw and Chemically Desulphurized Coals," Fuel, 62(9), 1070-1075 (1983).
8. R. Markuszewski, X. Zhou, and W. E. Straszheim, "Characterization of Sulfur Forms in Coal by Oxidative Degradation," in Processing and Utilization of High-Sulfur Coals IV, P. R. Dugan, D. R. Quigley, and Y. A. Attia, eds., Amsterdam, Netherlands, 1991, pp. 43-54.

DETERMINING MOLECULAR WEIGHT DISTRIBUTIONS OF POLAR COAL DERIVED LIQUIDS BY MEANS OF COMBINED GC/MS AND VACUUM TG TECHNIQUES

Huaying Huai and Henk L.C. Meuzelaar
Center for Micro Analysis & Reaction Chemistry
University of Utah, Salt Lake City, UT 84112.

Keywords: molecular weight distribution of coal liquids, gas chromatography/chemical ionization mass spectrometry, vacuum thermogravimetry

BACKGROUND

A novel, low temperature (<300 C) coal liquefaction method described by Shabtai et al. [1], consisting of a mild hydrotreatment (HT) step followed by base-catalyzed depolymerization (BCD) is thought to proceed by selective scission of C-C and C-O type bonds in the bridges connecting the aromatic and hydroaromatic clusters making up the bulk of the coal matrix, while minimizing secondary condensation reactions. Consequently, the resulting liquid products are expected to consist primarily of "monomeric" building blocks of the type and size inferred from solid state NMR measurements [2], i.e., corresponding to (hydro)aromatic structures with 10-15 aromatic carbons, 2-3 aliphatic carbons and 1-2 substituted oxygens (in addition to more sporadic sulfur, nitrogen or metal substituents) depending on coal rank, maceral composition, depositional environment and weathering status. In agreement with these expectations, the cyclohexane soluble "oil" fractions of the HT-BCD product, comprising up to 70% of the daf coal, were found to be completely vacuum distillable and to contain significant quantities of volatile, low MW components when analyzed by combined gas chromatography/mass spectrometry (GC/MS).

In order to further verify the mechanistic assumptions underlying the HT-BCD method as well as to obtain valuable information regarding type and size of the monomeric building blocks in coals, we decided to determine the precise molecular weight distribution (MWD) of HT-BCD oil fractions. The term MWD will be used interchangeably here with MMD (molecular or molar mass distribution). In view of the relatively low molecular weight and high polarity of the HT-BCD oil fractions, the use of gel permeation chromatography (GPC), also referred to as size exclusion chromatography [3], techniques was rejected in favor of mass spectrometry (MS) using "soft ionization" methods, such as field ionization (FI) and chemical ionization (CI), which tend to produce little or no fragmentation of molecular ions. Direct probe FIMS measurements were performed by Dr. H.R. Schulten (Fresenius Institute, Wiesbaden, GFR) whereas CIMS analyses were carried out in our laboratory using on-line prepreparation by short column capillary gas chromatography (GC) and sample injection by means of Curie-point flash evaporation. Well-known shortcomings of MS techniques include: possible loss of volatile components during sample introduction (in particular during direct probe MS); incomplete transport of low volatile components into the ion source (especially when using GC/MS); compound dependent response differences; and inability to analyze nonvolatile residues. Therefore, vacuum thermogravimetry (VTG) was selected as a tool for quantitative calibration, similar to its well established use for calibrating simulated distillation (SIMDIS) methods [4]. The results of these DP-FIMS, GC/CIMS and VTG experiments with a mixture of coal liquid like model compounds as well as with HT-BCD oil fractions from three ANL-PCSP (Argonne National Laboratory - Premium Coal Sample Program) coals, viz. Beulah Zap lignite, Illinois #6 hvCb and Blind Canyon hvBb coals, will be reported here.

RESULTS AND DISCUSSION

Since VTG showed each of the three HT-BCD oil samples to be completely vacuum distillable below 300 C without signs of degradation (Figure 1) we first attempted to determine the respective molecular weight distributions by means of DP-FIMS. As shown in Figure 2, MWD profiles obtained by DP-FIMS indicated apparent number average MW (MW_n) values in the 370-400 Dalton range. Considering the expected size of the molecular building blocks, e.g., 200-300 Daltons, these MW_n values were thought to be rather high.

Since direct probe introduction methods in MS are prone to loss of volatile components, a short capillary GC column operating at high linear flow velocities was used as a sample introduction device instead. Due to the unavailability of a GC/FIMS system, CIMS became the method of choice at this point. The advantages of using short capillary GC columns at high linear flow velocities over more conventional GC conditions are illustrated in Figure 3. Also note the effectiveness of isobutane Cl in minimizing fragmentation of molecular ions in comparison with the standard electron ionization technique. GC/CIMS data were obtained with a Finnigan MAT ion trap detector (ITD) type MS system. Comparison of the summed DP-FIMS and GC/CIMS spectra of Illinois #6 HT-BCD oil in Figures 2b and 3c, respectively, shows marked differences in observed ion distribution profiles. Obviously, the FIMS spectra suffer from a relative lack of low mass signals, presumably due to evaporation losses, whereas the GC/CIMS profiles lack some of the higher MW signals shown by FIMS, apparently due to a minor loss of heavy ends unable to pass through the short GC column.

Notwithstanding the discrepancies between the DP-FIMS and CIMS profiles, both types of profiles display a highly similar temperature dependence of avg. MW values (see Figure 4) except in the low MW part of the FIMS profile. However, as can be seen in Figure 2, the low MW part of the FIMS profile is entirely made up of low intensity mass peaks, apparently representing small quantities of residual oil remaining after evaporative loss of the lower ends. Consequently, the low MW part of the DP-FIMS curve is less reliable. Figure 5 demonstrates the temperature windowing technique used to calculate average MW values from temperature resolved MS data.

Considering the obvious differences in experimental conditions between the direct probe FIMS and the Curie-point vaporization GC/CIMS techniques the observed high degree of similarity in MW_n /Temp relationships merits some discussion. Because partial vapor pressures of individual compounds are independent of total pressure any apparent differences in temperature dependent behavior between the two systems must be due to intermolecular interactions and/or to transport limitations. Since high vacuum FIMS conditions resemble those of molecular distillation processes both effects are minimized and molecular size (as defined by the so-called "exclusion volume" [5]) becomes the dominant factor. Similarly, the Curie-point flash evaporation method used in GC/CIMS analysis effectively reduces the effect of intermolecular interactions by briefly elevating the sample to relatively high temperatures. Furthermore, the low effective sample concentrations in the gas and liquid phase, the chemical inertness of the fused silica capillary GC columns, the nonpolar poly(dimethyl/silicone) coating, the high linear carrier gas flow velocities and the short residence times combine to reduce intermolecular interactions and minimize transport limitations in the GC/CIMS system. Experimental support for these arguments can be found in the observation that capillary GC elution temperatures of petroleum crudes closely resemble vacuum distillation temperatures at 10 mm Hg [6]. Naturally, since kinetic considerations predict a strong heating rate dependence for apparent distillation and elution temperatures, it is important to use comparable heating rates in both experiments. Fortunately, heating rate is one of the most readily adjustable experimental parameters. Therefore, remaining temperature differences between desorptions, distillation or elution techniques may effectively be minimized by small adjustments in heating rate.

In order to transform the established MWn/Temp relationship into a molecular weight distribution, i.e., MWn/Weight Fraction relationship, we need to determine a reliable Weight Fraction/Temp relationship. In other words: what fraction of the sample (whether expressed as number of molecules or fraction of weight) is distilled, desorbed or eluted over each temperature interval?. This was measured by synthesizing a standard mixture consisting of known quantities of 87 coal-liquid like model compounds. In view of the unavailability of many possible coal liquid components any such mixture constitutes at best an approximation of a true coal liquid. Nevertheless, as shown in Figure 6, the observed MWn/Temp relationship (using GC/CIMS) is closely similar to that seen in Figure 4 (maximum avg. MW difference in 100-300 C range ≤ 10 Daltons). This encourages the further use of this model mixture to establish a Distillation Weight Fraction/Temp relationship by means of VTG (Fig. 7). As shown in Figure 7 the VTG curve (at approx. 5 mm Hg) closely follows the response corrected GC elution curve obtained at similar heating rate. By contrast, the ambient pressure ("transport limited") TG curve differs substantially from the vacuum TG profile.

Combination of the MW/Temp relationship (Figure 6) with the Weight Fraction/Temp relationship (Figure 7) produces the calculated Weight Fraction/MW relationship (=Molecular Weight Distribution) shown in Figure 8. Comparison with the known MWD of the model compound mixture in Figure 8 appears to confirm the validity of the combined GC/CIMS annex VTG approach.

In order to perform a more detailed analysis of the underlying relationships between average MWs and GC elution temperatures and to compare these with the atmospheric boiling point (ABP)/Elution Temp relationship used in SIMDIS [6] a smaller subset of 28 model compounds was selected for which ABP data are available in the literature. As shown in Figure 9, both correlations are of comparable strength ($r=0.990$ for ABP vs. temp., Figure 9a, with $r=0.985$ for MW vs. temp. Figure 9b), provided that n-alkanes are excluded from the model compound set in both cases. The anomalous behavior of n-alkanes in SIMDIS has been documented before [6]. As might be expected, the weakest correlation is found between ABP and MW (Figure 9c, $r = 0.971$). Intermolecular forces play a major role in determining ABP's without affecting MW values [7]. The fact that GC elution temperatures and MW values do not exhibit a perfect correlation does not necessarily argue against our prior assumption that under the special GC conditions used in our experiments (flash evaporation, high linear flow velocities, and short capillary column with inert walls and nonpolar coating) molecular exclusion volume may be the rate determining parameter. Exclusion volumes, although directly related to MW, are obviously influenced by other molecular properties as well. Unfortunately, exclusion volume values for the model compounds used were not available at the time of writing.

Application of the above described combined approach to the HT-BCD oils of the three ANL coals produces the three MW/Elution Temp. relationships shown in Figure 10. In agreement with the model data, all three coal liquids produced highly similar profiles in spite of significant differences in chemical composition. Most importantly, the calculated linear regression fit for the average slope and offset of the MW/Elution Temp relationship obtained for the model compounds shows an excellent fit with the coal liquid data as well. Finally, calibration of the relationship in Figure 10 with the measured vacuum TG profiles in Figure 1 results in the calculated MWD profiles shown in Figure 11. Note that the calculated average MW values, as well as the small but significant shift between the three coal liquids appear to be in line with the previously discussed assumptions regarding the type and size of key building blocks in coals of low to medium rank.

CONCLUSIONS

1. Short capillary GC columns operating at high linear flow velocities (facilitated by keeping the column outlet at vacuum pressure) produce elution temperature data which correlate closely with molecular weight for a broad selection of alkyl- and/or heteroatom substituted aromatic and hydroaromatic compounds. Correlation with vacuum TG data on fractional weight loss as a function of distillation/desorption temperature enables calculation of mass corrected MWD profiles. Based on the strength of the observed correlations, the error of the calculated MW values is expected to be well within $\pm 5\%$, which compares favorably with the reported accuracy of GPC based techniques for polar coal liquids [8].

2. For more or less strongly related coal-derived liquids, e.g. produced by the same liquefaction procedure, the observed relationship between avg. MW and elution temp. appears to be stable enough to eliminate the need for frequent recalibration by GC/CIMS (or GC/FIMS) techniques. Thus, a single vacuum TG determination under standardized conditions appears to be the method of choice for calculating reliable MWD profiles (provided that any significant quantities of n-alkanes are separated out before the measurement). For vacuum distillable coal liquids of unknown overall composition development of an on-line TG/MS technique (using FI or CI) may well provide the most direct approach to quantitative determination of MWD profiles (as long as excessive losses of volatile components are avoided).

3. Cyclohexane soluble "oil" fractions obtained from ANL coals of low to medium rank by means of low temperature HT-BCD were found to consist of molecular building blocks of a size and type which closely agree with solid state NMR data. Presumably, coal-derived liquids showing much larger average MW values (such as commonly seen in the coal liquefaction literature) must represent either: (a) high MW subfractions; (b) incompletely depolymerized fractions; (c) secondary recombination products; (d) retrograde reaction products; or (e) biased analytical procedures.

4. Arguably, MWD profiles provide a better yardstick for measuring the conversion efficiency of a given coal liquefaction process than solubility based parameters since the latter correlate poorly with molecular size and, thus, with the degree of depolymerization achieved.

ACKNOWLEDGEMENTS

The authors wish to thank H.R. Schulten, K. Holbrook, M. Statheropoulos and J.S. Shabtai for their highly valuable advice and kind help. This work was supported by the Consortium for Fossil Fuel Liquefaction Science (U.S. DOE) and by the Advanced Combustion Engineering Research Center NSF, State of Utah, 23 industrial participants and U.S. funded by DOE.

REFERENCES

1. Shabtai, J.S.; Saito, I. U.S. Patent 4,728,418, issued Mar. 1, 1988.
2. Solum, M.S.; Pugmire, R.J.; Grant, D.M. *Energy & Fuels*, 1989, 3, 187.
3. Evans, N.; Haley, T.M.; Mulligan, M.J.; Thomas, K.M. *Fuel*, 1986, 65, 694.
4. Southern, T.G.; Iacchelli, A.; Cuthiell, D.; Selucky, M.L. *Anal. Chem.*, 1985, 57, 303-308.
5. Perry, E.S. "Distillation under High Vacuum", in: *Distillation*, E.S. Perry and A. Weissberger (eds.), Interscience Publishers, Chapter V, 1965, pp. 535-551.
6. Annual Book of ASTM Standards, 1988, Vol. 05.02, pp. 506-513.
7. Boduszynski, M.M. "Limitations of Average Structure Determination for Heavy Ends in Fossil Fuels" in: *Liquid Fuels Technology*, 1984, 2(3) pp. 211-232.
8. Bartle, K.D. "Chromatographic Techniques" in: *Spectroscopic Analysis of Coal Liquids*, J.R. Kershaw (ed.), 1989, pp. 13-40.

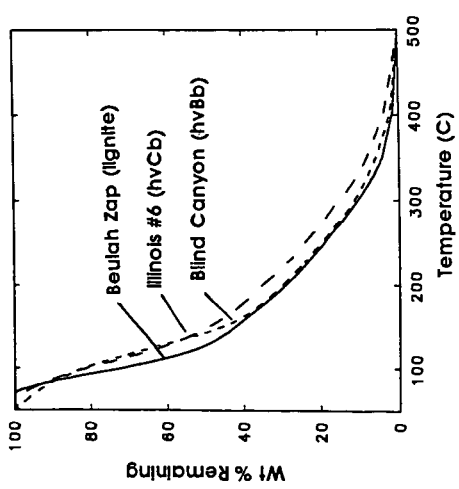
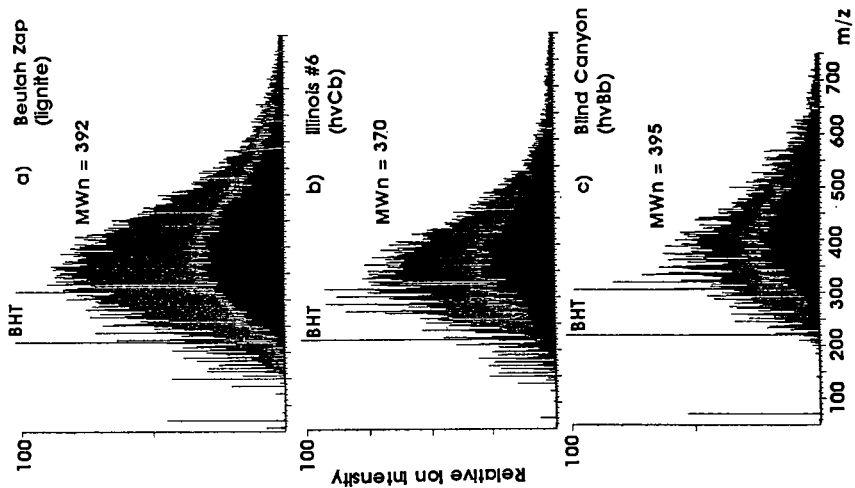


Figure 1. Vacuum TG curves for three HT-BCD oils.

Figure 2. Direct probe field ionization MS profiles for three HT-BCD oils. Note BHT (dibutylhydroxytoluene stabilizer residue from THF extraction) at m/z 220.

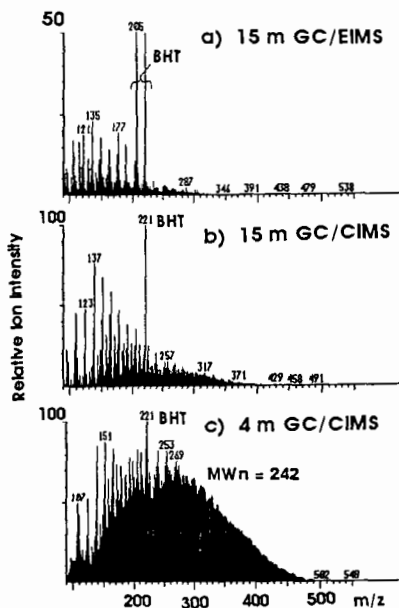


Figure 3. Effect of column length (15 m vs. 4 m) and ionization method (EI vs. CI) on ion distribution profiles of Illinois #6 HT-BCD oil.

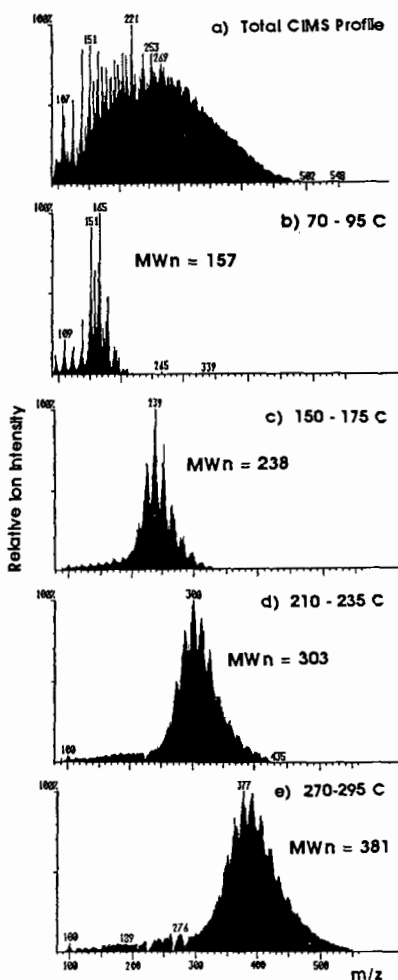


Figure 5. Temperature window (25 C) technique used to calculate avg. MW/Temp relationship data illustrated for GC/CIMS profile of Illinois #6 HT-BCD oil.

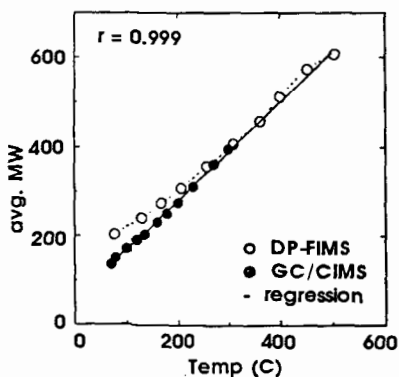


Figure 4. Comparison of avg. MW/Temp relationships observed by DP-FIMS and GC/CIMS analysis of Illinois #6 HT-BCD oil.

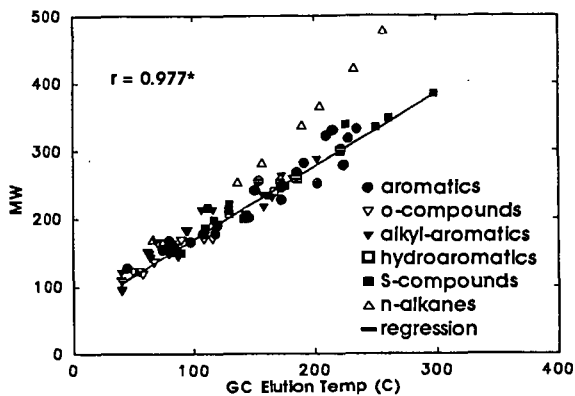


Figure 6. Observed MW/GC elution temperature relationship for a mixture of 87 model compounds. *n-alkanes removed from regression calculation.

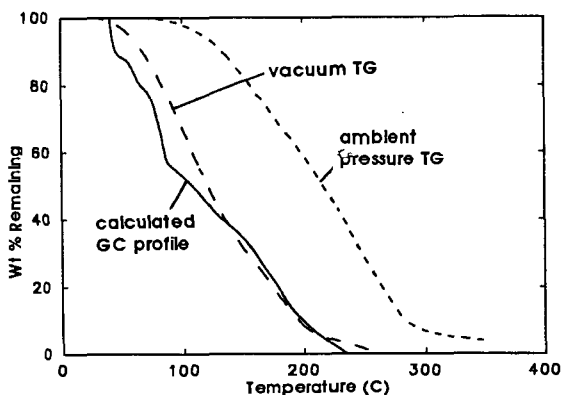


Figure 7. Comparison between Temperature-Fraction Weight loss relationships obtained by vacuum TG and ambient pressure TG of a mixture of 87 model compounds, as well as by weight corrected, integrated GC elution profiles.

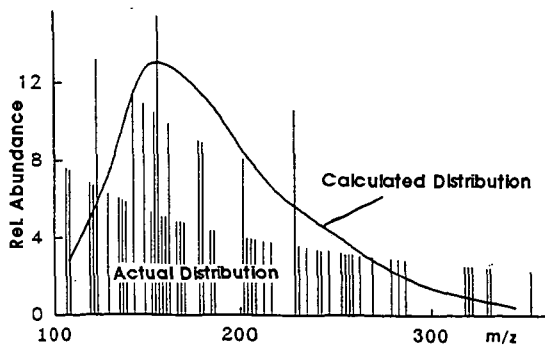


Figure 8. Comparison between calculated MWD and actual MWD of model compound mixture.

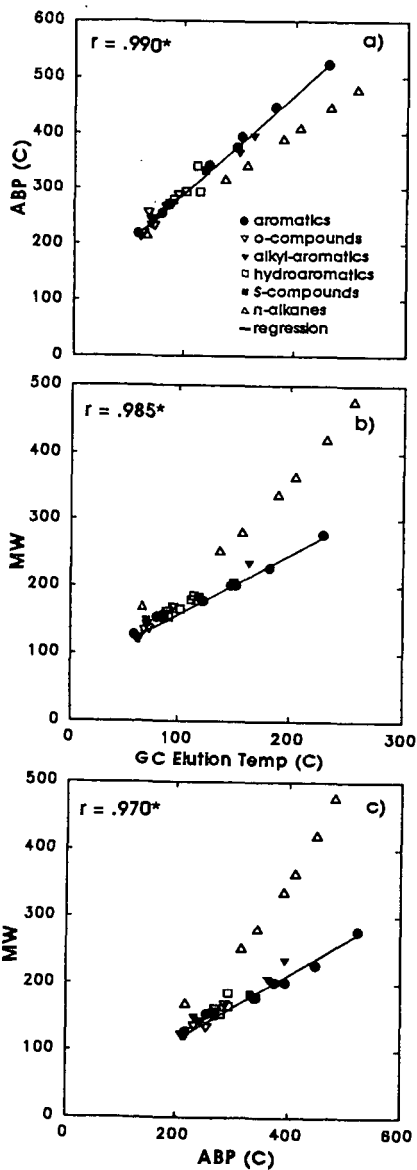


Figure 9. Observed correlations between ABP (Atmospheric Pressure Boiling Point), MW and GC elution temperature for a subset of 28 selected model compounds. n-alkanes removed.

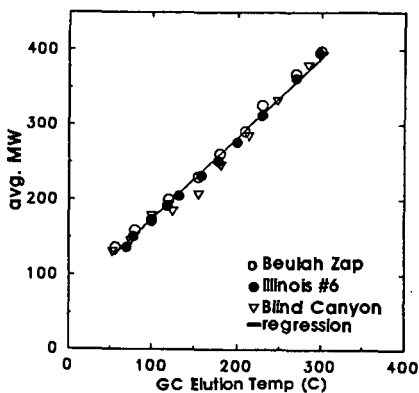


Figure 10. Comparison between observed avg. MW/GC elution temp relationships for three HT-BCD oils and the predicted regression line obtained from the 87 model compound mixture.

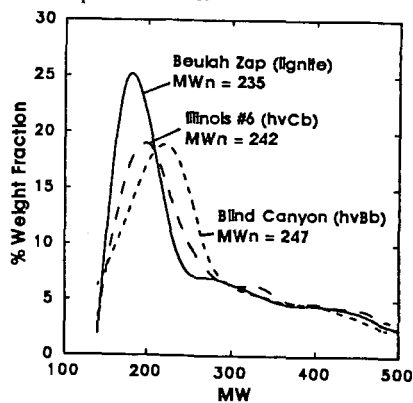


Figure 11. Calculated MWD curves for the three HT-BCD oils. Note slight increase in MW_n as a function of rank.